Journal of Applied Polymer Science

The flame-retardant properties and mechanisms of poly(ethylene terephthalate)/hexakis (para-allyloxyphenoxy) cyclotriphosphazene systems

Jiawei Li, Feng Pan, Xiandong Zeng, Hong Xu, Linping Zhang, Yi Zhong, Xiaofeng Sui, Zhiping Mao
Key Laboratory of Science and Technology of Eco-Textile (Ministry of Education), Donghua University, Shanghai 201620, People's Republic of China
Correspondence to: H. Xu (E-mail: hxu@dhu.edu.cn) and Z. Mao (E-mail: zhpmao@dhu.edu.cn)

ABSTRACT: Para-allyl ether phenol derivative of cyclophosphazene (PACP) was prepared and used as a filler to modify the flame-retardant properties of poly(ethylene terephthalate) (PET) by melting-blending. The mechanism of flame-retardant was discussed and the influences of flame-retardant contents to the mechanical properties were studied. The results revealed that the incorporation of only 5 phpp PACP (0.37 wt % phosphorus containing) into PET matrix can distinctly increase the flame retardancy of PET/PACP composition, and it has a little effect on the mechanical properties of PET. The high flame-retardant performance of PET/PACP composite was attributed to the combination of condensed-phase flame retardant and gas-phase flame retardant. © 2015 Wiley Periodicals, Inc. J. Appl. Polym. Sci. **2015**, *132*, 42711.

KEYWORDS: composites; flame retardance; mechanical properties; polysters; thermal properties

Received 15 April 2015; accepted 6 July 2015
DOI: 10.1002/app.42711

INTRODUCTION

Organophosphate esters (OPEs) as a kind of useful flame retardant (FR) for poly(ethylene terephthalate) (PET) fabric gained extensive manufacture and application even increase due to the ban of halogen containing FR.[1–5] Unfortunately, the diffusion from host materials result in continuous release of OPEs and their distribution through water, especially wastewater, and air, particularly associated with airborne particulate matter.[5–9] Furthermore, some of OPEs is labeled as a potential carcinogenic substance during the living organisms long-term exposure.[8] Therefore, the development of nonhalogen, low toxicity, eco-friendly, and high-efficiency FR becomes a real challenge for both scientific and industrial fields.

When the additive FRs are physically incorporated into PET matrix, the mechanical properties of composites could be reduced, which restricts the application of most commercially available additive-type FRs.[10–13] To overcome this problem, improving the flame-retardant efficiency of FRs is a alternative way to decreasing the content of FRs in the polymer matrix. By this way, it can enhance mechanical and other properties of flame-retardant PET.[10] The bi-phase flame-retardant activity of phosphorous compounds showed the high flame-retardant efficiency.[9,14–16] The flame-retardant activity in the condensed phase creates a charred layer by dehydration and further cross-linking reactions. The activity in gaseous phase releases such as PO, PO_2, and HPO·which scavenge free radicals OH· and H· responsible for the spread of flame.

Cyclotriphosphazene derivatives (CPs) is a dramatically high efficiency in flame retardancy because of the synergistic effect of the skeletal phosphorous and nitrogen element in the phosphazene ring.[17,18] One subgroup of these CPs containing carbon-carbon unsaturated groups, were found to enable copolymerisation with other organic polymer,[3] such as unsaturated polyesters,[19] polystyrene,[20,21] polycarbonate,[22] and polymethyl methacrylate,[23] to improve the thermal stability and flame retardance of composites. However, the low reaction activity between the unsaturated groups and PET during the process of polycondensation limits its application as a flame retardant for PET.

It was well known that allyl ethers derivatives of organic compounds are capable for rearrangement and could not be homopolymerized by a radical mechanism in the heat condensation. Bagnell *et al.*[24] also reported that the Claisen rearrangement products of allyl phenyl ether under 290°C neat condition were constituted by 87% 2-allylphenol, 7% 2-methyl-2,3-dihydrobenzofuran, 3% phenol and 3% isomeric 2-(prop-1-enyl)phenols. The more thermally stable exothermic Claisen rearrangement CP products (such as 2-methyl-2,3-dihydrobenzofuran) could lead to the formation of rich char residues,

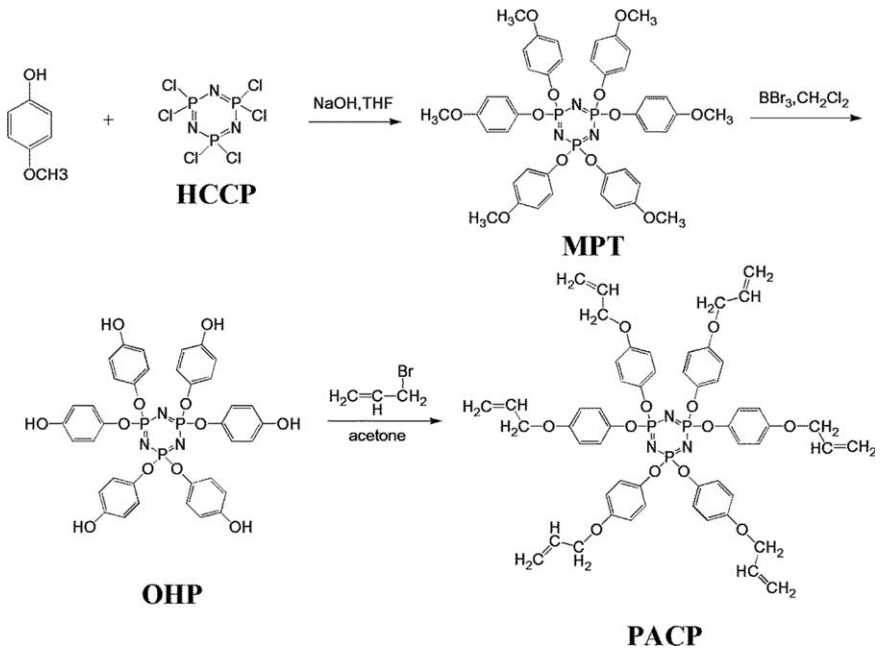

Scheme 1. The synthesis route of hexakis(4-allyloxyphenoxy) cyclotriphosphazene (PACP).

which are beneficial to enhance the flame-retardant efficiency of FR.[24,25] Para-allyl ether phenol derivative of cyclophosphazene (PACP, Hexakis(para-allyloxyphenoxy) cyclotriphosphazene) was reported to be used to prepare the epoxy derivatives to open up the practical exploitation of phosphazene matericals.[26] Up to now, to the best of our knowledge, hardly is there a report on PACP utility as FR for PET.

In this article, PACP is expected to act as a high-efficiency FR to modify the PET matrix at lower content and can limit detrimental effect on the mechanical properties for the resins to an acceptable level, since PACP contains the para-allyl ether phenol groups which could thermal rearrangement during melt-blending process. The flame-retardant effects, mechanisms and mechanical properties of PET/PACP composites were discussed in details.

EXPERIMENTAL

Materials

The hexachlorocyclotriphosphazene (HCCP) (Zibo, LanYin Chemical) was purified from hot n-heptane and dried *in vacuo* at 60°C under −0.1 MPa. 4-Methoxypheol, boron tribromide, NaOH, K_2CO_3, tetrahydrofuran (THF), dichloromethane, acetone, and ethyl acetate were all purchased from Shanghai Chemical Agent Company. PET (FG 600, $[\eta] = 0.675$ dL/g) was provided by Sinopec Yizheng Chemical Fibre.

Synthesis of Hexakis(para-allyloxyphenoxy) cyclotriphosphazene, PACP

Para-allyl ether phenol derivative of cyclophosphazene (PACP) was prepared according to the literature,[26,27] by three-step synthetic method, as shown in Scheme 1. First, synthesis of $N_3P_3(OC_6H_4\text{-}p\text{-}OCH_3)_6$ (MPT), HCCP (1.0 g, 2.87 mmol), 4-methoxypheol (2.48 g, 20 mmol), NaOH (0.96 g, 24 mmol) and 24 mL THF were refluxed in a glass flask for 24 h. Second, synthesis of $N_3P_3(OC_6H_4\text{-}p\text{-}OH)_6$ (OHP), the deprotection of $N_3P_3(OC_6H_4\text{-}p\text{-}OCH_3)_6$ (2.18 g, 2.5 mmol), was used by boron tribromide (1.74 mL, 18.4 mmol) in CH_2Cl_2 (30 mL) for 48 h at room temperature. Third, synthesis of $N_3P_3(OC_6H_4\text{-}p\text{-}O\text{-}CH_2\text{-}CH{=}CH_2)_6$ (PACP), a mixture of $N_3P_3(OC_6H_4\text{-}p\text{-}OH)_6$ (0.79 g, 1 mmol), allyl bromide (0.76 mL, 9 mmol), and K_2CO_3 (0.83 g, 6 mmol) was refluxed in 30 mL acetone for 16 h. After evaporated the solvent under reduced pressure, the residue was dissolved in ethyl acetate and washed with 10% NaOH solution and water. The yellow viscous liquid was obtained, yield 57.3%, after drying the organic layer with anhydrous sodium sulfate and evaporating it to a constant weight in vacuum at 60°C under −0.1 MPa.

Preparation of PET/PACP Composites

PET pellets and PACP were dried in a vacuum oven at 140°C under −0.1 MPa for 24 h before use. The PET pellets mixed with different contents of PACP respectively [5, 10, and 15 per hundred parts polyol (phpp)] at 80 rpm for 8 min at 280°C using a Haake Rheocord 90 internal mixer. Then, without dried treatment, those samples sequentially injected into bars for the LOI value, UL 94 test, and the mechanical experiment, via a miniature injection machine (Model DHS-5, Shanghai, China). The injection pressure, temperature, and time were chosen as 3 MPa, 280°C, and 30 s, respectively. The mold temperature was set at 40°C.

Measurements

Fourier transform infrared (FTIR) and Real-time Fourier transform infrared spectroscopy (RT-FTIR) were performed on an Avatar 380 FTIR (Thermo Electron, USA) spectroscope. ^{1}H-NMR, ^{31}P-NMR, and ^{13}C-NMR spectra were collected on a Bruker Avance Spectrometer (400 MHz). ^{13}C solid-state NMR were measured at room temperature. The recycle time was 4 s, and the spinning rate was 5 KHz. Thermogravimetric analysis

(TGA) was carried out with a TG 209 F1 thermal analyzer (NETZSCH, Germany) from 35 to 900°C at a heating rate of 10°C/min under both nitrogen and air atmosphere. Differential scanning calorimeter analysis (DSC) was conducted on a DSC 204 F1 thermal analyzer (NETZSCH, Germany). To analyze the thermal reaction behavior, the sample was scanned twice from 30°C to 280°C. To investigate the crystallization behavior, the samples were heated from 30°C to 280°C and kept 280°C for 5 min to eliminate their thermal history, then cooled to 30°C and reheated to 280°C, respectively. All the DSC tests were at a heating rate of 10°C/min under nitrogen atmosphere. Pyrolysis-gas chromatography-mass spectrometry (Py-GC/MS) tests were recorded with a system consisting of a FRONTIER P-2020iD Pyrolyzer and a SHIMADZU GC-MS QP2010, and the carrier gas was helium. Scanning electron microscopy (SEM) observations were carried out using a Hitachi TM-1000 scanning electron microscope.

Elemental Analysis (EA) of carbon and nitrogen was analyzed using an Elmentar Vario EL III (Germany) according to the JY/T 017–1996. Determination of the amounts of carbon was made by burning the sample in an excess of oxygen at 1000°C, then determined the evolved CO_2. The quantity of nitrogen was determined by burning the sample in He with 3% oxygen at 1000°C, then determined the evolved nitrogenated oxides. The phosphorous content of PET/PACP composites was analyzed using an Leeman Prodigy (USA) Inductively Coupled Plasma-Atomic Emission Spectrometry (ICP-AES) according to the JY/T 015–1996. Samples were digested with a mixture of H_2SO_4, HNO_3, and H_2O_2, and then ICP-AES was used to the determination of phosphorus by choosing the spectral line of 214.914 nm as analytical line.

The combustion behavior was investigated by Govmark MCC-2 microscale combustion calorimeter (MCC, USA) according to the ASTM D7309-11. The LOI values were measured on the Oxygen Index Flammability Gauge (ATS 1004050, ATS FAAR, Italy) according to the ASTM D 2863. Samples were molded to a size of 125 mm × 6.5 mm × 3.2 mm through injection molding. The UL 94 vertical burning tests were evaluated according to the ANSI/NL 94-2013 testing procedure. The text samples had a size of 125 mm × 12.5 mm × 3.2 mm. The tensile properties of composites were measured with a H10k-S (Tiniius Olsen, American) materials universal testing machine at a constant cross-head speed of 1 mm/min. All of the tests were carried out at room temperature, and the values reflected an average from five tests.

RESULTS AND DISCUSSION

Synthesis and Exothermic Claisen Rearrangement of PACP

The synthetic process of PACP was tracked by FTIR and NMR. The results are shown in Figure 1. As shown the FTIR spectra of MPT, OHP, and PACP in Figure1(A), peak at 1182 cm^{-1} was attributed to the stretching vibration absorption of P═N in the cyclotriphosphazene ring skeleton; 1060 cm^{-1} and 945 cm^{-1} were assigned to P—O—Ph vibration, suggesting that the synthetic material contained phosphorous nitriles matrix and replaced by the phenol derivative. Moreover, the FTIR spectra of PACP showed new stretching vibration of C═C (1646 cm^{-1}),

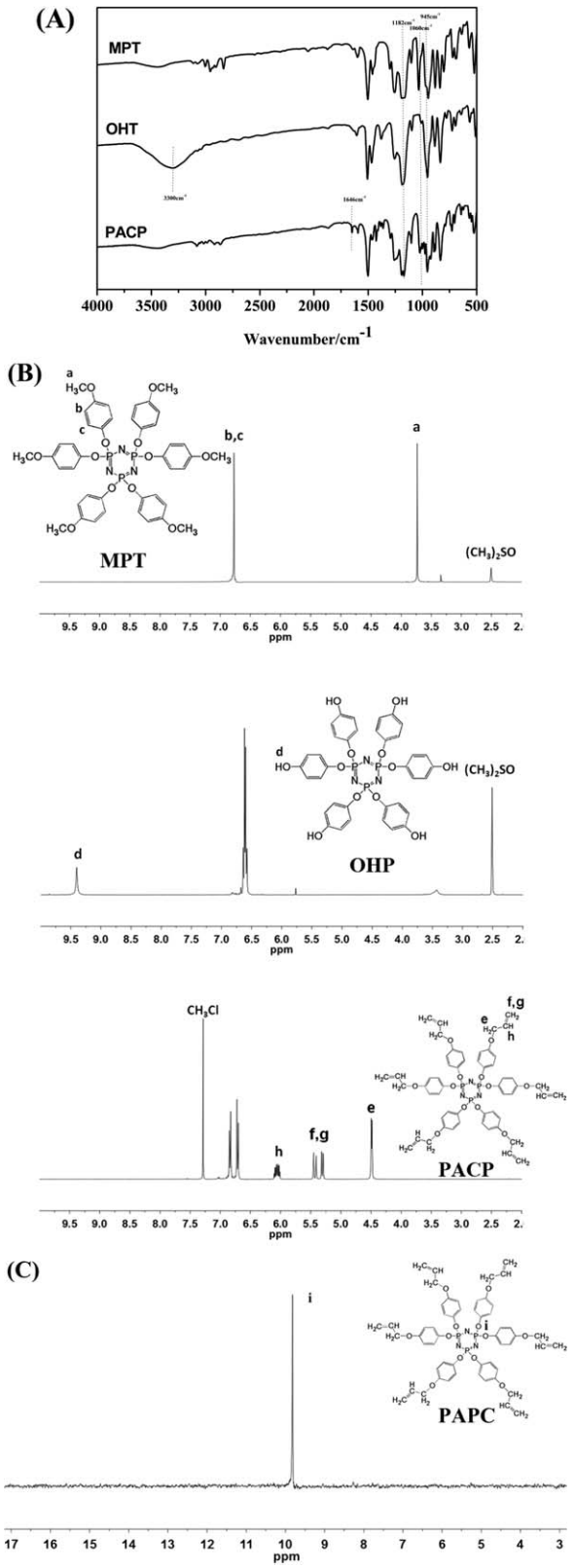

Figure 1. FTIR spectrum of MPT OHP and PACP (A), ^{1}H-NMR spectrum of MPT OHP and PACP (B) and ^{31}P-NMR spectra of PACP (C).

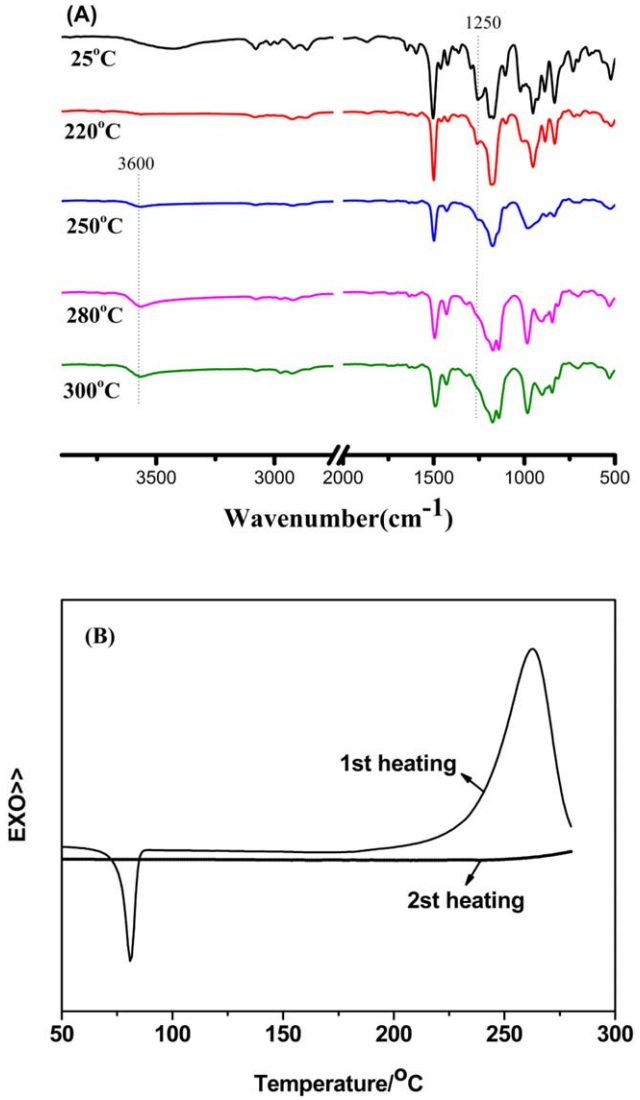

Figure 2. Dynamic FTIR spectrum (A) and DSC (B) of PACP. [Color figure can be viewed in the online issue, which is available at wileyonlinelibrary.com.]

which indicated that the unsaturated double bonds of PACP functional groups.[19,22]

The structure of PACP was also characterized by ^{1}H-NMR and ^{31}P-NMR. Figure 1(B) showed ^{1}H-NMR the spectra of MPT, OHP, and PACP. There were two peaks at 3.75 ppm (-OCH_3, denoted a) and 6.87 ppm (-C_6H_4-, denoted b, c), as shown in Figure 1(B), which indicated the chemical structure of MPT. The signal at $\delta = 9.41$ppm was ascribed to peak of the phenol protons of the OHP (-C_6H_4-OH, denoted d) and the methoxy protons peak ($\delta = 3.75$ ppm) completely disappeared, which suggested the all deprotection procedure of MPT accomplished.[27] Three signals at $\delta = 4.48$ppm (—CH═, denoted e), $\delta =$ 5.25-5.5ppm (—CH═CH_2, denoted f, g) and $\delta =$ 6.05ppm (—CH_2—CH═, denoted h) was caused by allyl ether groups of PAPC.[26] On the other hand, the complete substitution of phenol in OHP could be indicated by the singlet signal [as shown in Figure1(C)] in the ^{31}P-NMR spectrum of PACP. Those changes in chemical shift proved that the flame-retardant PACP was successfully synthesized.

The exothermic Claisen rearrangement of PACP was examined by the real-time FTIR under air atmosphere and DSC under N_2 atmosphere and the corresponding results are showed in Figure 2. Figure 2(A) shows the chemical structure changes in RT-FTIR spectrogram at different temperature in KBr disk. When the temperature raised to 250°C, the appearance of band at 3600 cm^{-1} was attributed to phenolic hydroxyl groups and the stretching vibration of ether at 1250 cm^{-1} disappeared, which was caused by the exothermic Claisen rearrangement of allyl ether groups.[24,28,29] Additionally, thermograms were obtained by scanning the sample twice from 30°C to 280°C with a heating rate of 10°C min^{-1}. PACP displayed a sharp melt transition peak around 70°C and a broad exothermic peak for the exothermic Claisen rearrangement of allyl ether above 200°C in the DSC thermogram, as shown in Figure 2(B). Conversely, no significant exothermic peak appeared in the second scan. It was demonstrated that more thermally stable exothermic Claisen rearrangement CP products (such as 2-methyl-2,3-dihydrobenzofuran groups) were prepared by thermal reaction of PACP during the firstly scanning process.[24]

To further confirm the chemical structure of PACP, ^{13}C-NMR and solid-state ^{13}C-NMR characterized PACP and the sample after 280°C thermal treatment for 30 min, respectively, the corresponding spectrogram are showed in Figure 3. The typical resonance peaks of PACP disappeared at δ=69.0 ppm (Ph—O—CH_2—, denoted C_3), as shown in Figure 3, and the peaks at δ=38.0 ppm (Ph—CH_2—, denoted a, 3) appeared, which indicated that the ether bond completely broken and the exothermic Claisen rearrangement of PACP occurred during the thermal treatment process. Thus, the major rearrangement products of allyl ether groups on PACP were 2-methyl-2,3-dihydrobenzofuran or 2-allyphenol groups. 2-Allyphenol groups were capable of the etherification reactive between the phenolic hydroxyl groups with the terminal carboxyl of PET during the process of melt blending.[17]

Flammability Properties of PET/PACP Composites

The vertical burning tests (UL 94) and LOI values were used to investigate the flame retardancy of the samples and the results were listed in Table I. For PET/PACP samples, when the adding content of PACP reached to 5 phpp, the LOI value increased from 26.5 vol % (the LOI value for neat PET) to 33.5 vol %, but then, that of PET/15%PACP was 32.1 vol % as shown in Table I. It suggested that the PET/PACPs composites was not easy to be ignited and the more PACP incorporated into PET matrix did not increase the LOI values of the samples. Thus, PACP can endow the higher LOI values of materials.

During the vertical burning tests (UL 94), V-0 rating can be achieved when the average self-extinguished time is less than 10 s after both first and second 10 s application of the burner, as well as the underlying cotton pad is not ignited by the flaming drops.[30] In UL 94 test, the neat PET could not pass V-0 rating, no self-extinguishing in short time, and serious flaming melt drops ignited the underlying cotton pad. However, for the PET/PACP system, only 5 phpp PACP was introduced into the PET matrix, it could reach the V-0 rating during the UL 94 test. Compared with the neat PET, the PET/5%PACP exhibited

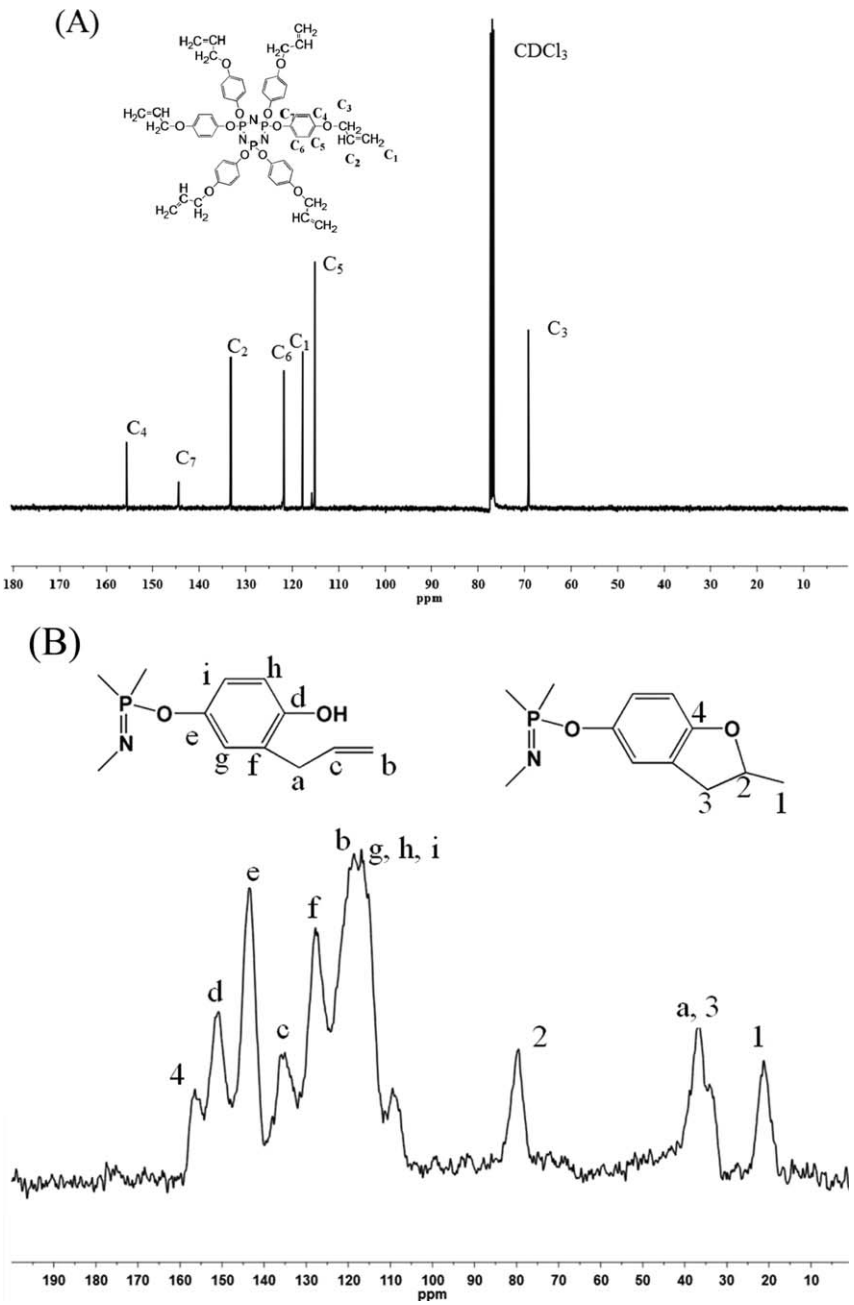

Figure 3. ^{13}C-NMR spectra of PACP (A) and ^{13}C MAS NMR spectra of PACP after 280°C treatment for 30min under air conditions (B).

Table I. LOI (vol %) Values and UL-94 of Neat PET and PET/PACP Samples

		Flammability from vertical burning testing			
Samples	LOI value (vol %)	UL-94 classification	Observed dripping[a]	Ignition the cotton	SET[b]
Neat PET	26.5	V-2	Drip/Drip	Yes	
PET/5%PACP	33.5	V-0	None/Little	No	0/0
PET/10%PACP	33	V-0	None/Drip	No	0/0
PET/15%PACP	32.1	V-0	Little/Little	No	0/0

[a] The first and second combustion dripping; Drip defined as above 2 drips, Little defined as 1–2 drips.
[b] Average self-extinguished time after the first and the second 10 s application of the burner.

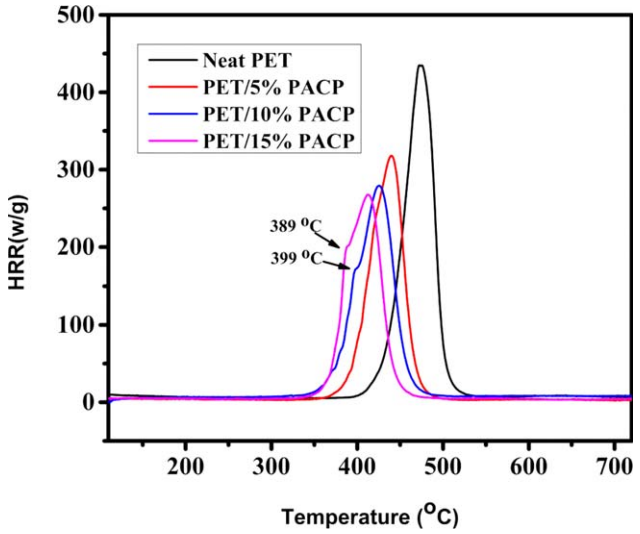

Figure 4. HRR curves of neat PET and PET/PACP composites. [Color figure can be viewed in the online issue, which is available at wileyonlinelibrary.com.]

high-effective self-extinguishment. The nonflaming melt drops were only to be observed in the second flame application. In order to provide the critical combustion information, such as peak heat release rate (PHRR), micro-sale combustion calorimetry (MCC) was used to evaluate the flammability parameters for neat PET and PET/PACP composites,[31] the results are shown in Figure 4 and the corresponding date is given in Table II. When the PACP concentration was increased from 0 to 15 phpp, as presented in Table II, PHRR of PET composites decreased from 428.2 W/g to 270.4 W/g, as well as the heat release capacity (HRC) from 427.3 KJ/g to 270.0 KJ/g. It was also observed that the temperature to PHRR (temp) and the total heat release (THR) decreased, and the yield of pyrolysis residue (YPR) increased as the PACP addition increased (seen in Table II). Figure 4 clearly showed the decrease of PHRR as a result of increase in the amount of PACP incorporated into PET matrix. Additionally, the two "shoulder" at 389 and 399°C for the curves of the PET/15%PACP and PET/10%PACP, respectively, which was caused by the decomposition of the flame-retardant (PACP) at lower temperature.[31] It was noticed that the PHRR of PET/5%PACP and PET/10%PACP were 313.9 and 271.6 W/g, which was lower than that of neat PET by 26.7% and 36.6%, respectively, while that of PET/15%PACP was reduced by 36.9%. This implied that the introduction of flame retardant (PACP) enhanced the fire safety of the polyester. One

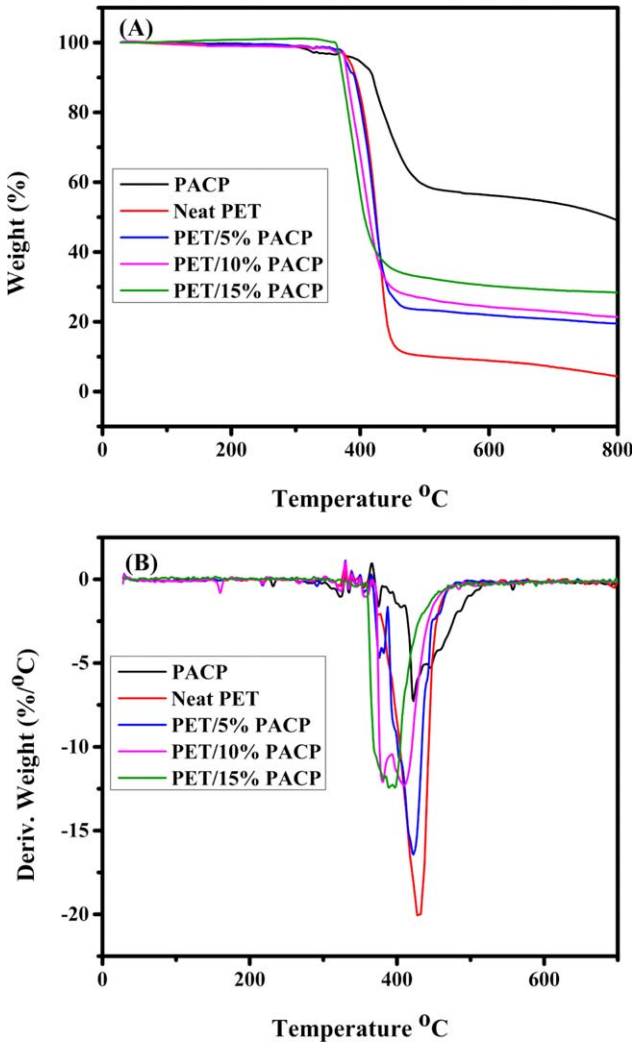

Figure 5. The TG (A) and DTG (B) curves of PACP, neat PET, and PET/PACP blends in nitrogen. [Color figure can be viewed in the online issue, which is available at wileyonlinelibrary.com.]

the other hand, when the volume addition was 15 phpp, the flame retardance of PET/PACP compositions was not the further enhanced.

Combining the analysis of LOI, UL 94, and MCC tests, it was clearly observed that the PACP possessed high efficiency of flame retardancy for PET. The distinct flame-retardant effects could be explained on the basis of the analysis of flame-retardant mechanism, especially thermal degradation, pyrolysis

Table II. Microscale Combustion Calorimeter Results

Sample	PHRR (W/g)[a]	THR (KJ/g)[a]	Temp (°C)[a]	HRC (KJ/g)[a]	YPR (g/g)[a]
Neat PET	428.2	18.7	474.3	427.3	0.08
PET/5%PACP	313.9	14.8	440.4	311.7	0.19
PET/10%PACP	271.6	14.2	424.1	270.7	0.23
PET/15%PACP	270.4	13.3	411.4	270.0	0.26

[a] PHRR, peak heat release rate; THR, total heat release; temp, temperature to PHRR; HRC, heat release capacity; YPR, yield of pyrolysis residue.

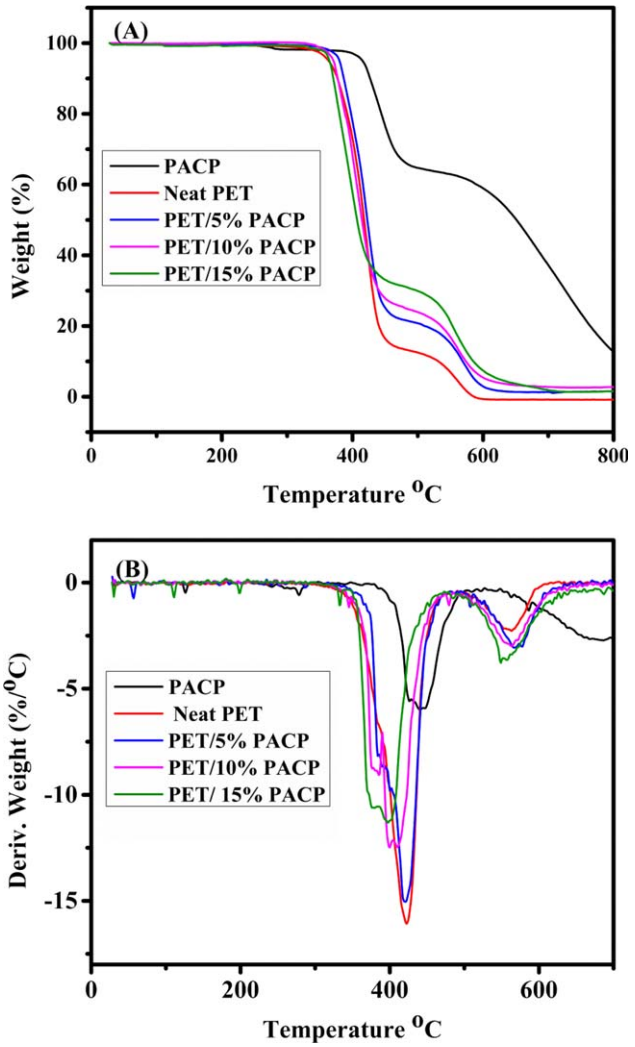

Figure 6. The TG (A) and DTG (B) curves of PACP, neat PET, and PET/PACP blends in air. [Color figure can be viewed in the online issue, which is available at wileyonlinelibrary.com.]

behavior and char residue morphology. The further mechanisms will be discussed later.

Thermal Properties of PET/PACP Composites

The thermal properties of PET, PACP and PET/PACP composites were tested under nitrogen and air atmosphere, as shown in Figures 5 and 6, the relevant data including the initial decomposition temperature ($T_{5\%}$), the temperature of maximum mass loss (T_{max}), the rate of the T_{max}, and the yield of the char residues at 800°C in nitrogen and air atmospheres are listed in Table III.

As demonstrated in Figure 5, the TGA curves presented typical one-stage decomposition in nitrogen atmosphere. The initial decomposition temperature of PACP ($T_{5\%}$) was 369°C, the sequent of T_{max} was 422°C, and a considerable amount of residue of PACP at 800°C was obtained, which was 49.01 wt %. The start degradation temperatures of PET/5%PACP was 377°C, lower than that of neat PET (382°C), resulted from the thermal decomposition of PACP. The maximum decomposition rate

Table III. TGA Data of the Blends in Nitrogen and in Air

	Under nitrogen atmosphere				Under air atmosphere				
						T_{max} (°C)		The rate of T_{max} (wt % min^{-1})	
Sample	$T_{5\%onset}$ (°C)	T_{max} (°C)	The rate of T_{max} (wt % min^{-1})	Residue at 800°C (wt %) (by measurement)	$T_{5\%onset}$ (°C)	Stage 1	Stage 2	Stage 1	Stage 2	Residue at 800°C (wt %) (by measurement)
Neat PET	382	428	20.1	4.35	363	423	563	16.1	2.3	0
PACP	369	422	7.3	49.01	415	441	726	5.98	2.8	12.57
PET/5%PACP	377	421	16.4	19.48	379	421	567	15.1	3.1	1.51
PET/10%PACP	376	409	12.3	21.35	369	410	563	12.5	3.0	2.73
PET/15%PACP	368	389	12.4	28.35	364	397	557	11.3	3.6	1.56

$T_{5\%onset}$ defined as the temperature at which 5 wt % weight loss occurred.
T_{max} defined as the temperature at maximum weight loss rate.

Table IV. Main Pyrolysis Products of PACP

PACP		
Time (min)	Products	Relative peak intensity (%)
8.866	Phenol	3.37
9.26	2-Propenal, 3-phenyl	6.58
9.866	Phenol, 3-methyl-	0.2
10.009	2-Methyl-2,3-dihydrobenzofuran	1.52
10.075	Benzofuran, 2-methyl-	0.43
10.171	Benzofuran, 4,7-dimethyl-	0.83
10.358	2-Allylphenol	36.6
12.045	Phenol, 4-2-propenyl)-	7.66
12.83	2H-1-B2nzopyran, 3,4-dihydro-	3.34
13.206	1,4-Benzendiol	8.45
13.377	2-Cyclohexen-1-one, 3-methyl-6-(1-methylethylidene)-	9.5
13.462	2-Methyl-5-hydroxybenzofuran	8.05
14.121	Bicyclo[2.2.2]octa-2,5-dine, 1,2,3,6-tetramethyl-	3.48
14.341	Benzaldehyde,2,4,6-trimethyl-	3.86
14.546	3-Buten-2-one, 4-(4-methoxyphenyl)-	3.92
16.189	Benzoic acid, 3,5-dimethyl-	2.21

decreased, as shown in Table III, when the adding amount of PACP increased from 0 phpp to 10 phpp. In addition, all of PET/PACP composites had higher char yields compared with neat PET, for instance, the yield of residual of PET/15%PACP with 28.35 wt % at 800°C, suggested that the composites performed better in charring at higher temperature.

Figure 6 shows the thermal oxidative degradation behaviors of PACP, neat PET, and PET/PACP composites under air atmosphere. Two-step degradation processes displayed in the TGA and DTG curves: one step was the thermal pyrolytic decomposition of PACP, neat PET, and PET/PACP composites, the other step was the reoxidation of the first step of degradation remaining char with the action of O_2 at higher temperature.[17,18,32,33] It was different that, the cure of PACP in air atmosphere, as the temperature raised above 600°C, showed a large amount of weight loss, indicating that the thermal stability of early degradation remaining char of PACP was relatively poor at high temperature. Similar with the TGA results of PET/PACP composites in N_2 atmosphere, the $T_{5\%}$ was also lower than that of neat PET under air atmosphere. The yield of the PET/PACP composites' residual char increased slightly from 0 wt % to 2.73 wt % with the increase of PACP content from 0 to 10 phpp, respectively. The calculated char residue of PET/10%PACP, for instance, by the weight ration of the residue at 800°C for neat PET and PACP, was 1.14 wt %. The enhancement of formed char was 1.59 wt % by taking off the calculated charred residue. This is, there were chemical reactions between PACP and PET matrix during the decomposition of the PET composites. But, as the increase of PACP to 15 phpp, the yield of residual char reduced to 1.56 wt %, which was lower than the calculated char residue (1.64 wt %). The same phenomenon was observed in our previous study of PET/HPAIPC system,[33] which implied that more PACP incorporated into PET could not promote the formation of more thermo-oxidative stability char layer in PET/PACP system, due to the degradation of PACP at high temperature. According to the thermal and thermo-oxidative decomposition behavior of PET/CPs composites, a conclusion could be concluded: during thermal and thermo-oxidative decomposition, the PAPC firstly decomposed to form phosphate and polyphosphate, promoted the formation of highly crosslinked and rigid char layer, leaded to PET/PACP composites with a good thermal stability.

Pyrolysis: Evolved Gas Analysis of PET/PACP Composites

In order to investigate the pyrolysis products of PACP and PET/PACP composites and speculate the flame retardance mechanism of the composites in gaseous phase, Py-GC/MS tests at 450°C were performed.

Table IV illustrates the pyrolysis products of PACP. The fragment flows with some characteristic ionic peaks of PACP illustrate in Figure 7. Obviously, a strong molecular ion peak was found at M/Z 94 (phenol) and the further decomposed fragments were generated, such as C_5H_6 at M/Z 66 and C_3H_3 at *M/Z* 39. Besides, it should be noticed that the *M/Z* value of 64 and 63 (HPO_2 and PO_2 free radical produced) appeared in the Figure 7, which was produced by the PO free radicals from the broken cyclotriphosphazene group combining with OH, H or O free radicals.[14] Those volatile phosphorus-containing flame retardants (PFRs) were considered that the most effective combustion inhibitors since phosphorus-based radicals were, at the same molar, five times more effective than bromine and 10 times more effective than chlorine radicals.[9] Thus, PET/PACP composites exhibited high flame retardancy and self-extinguishing during the LOI and UL 94 tests. On the other hand, the major pyrolysis products of PACP, as shown in Table IV, were 2-allylphenol, 1,4-Benzendiol, and 2-Cyclohexen-1-one, 3-methyl-6-(1-methylethylidene), etc. The volatile fragments of

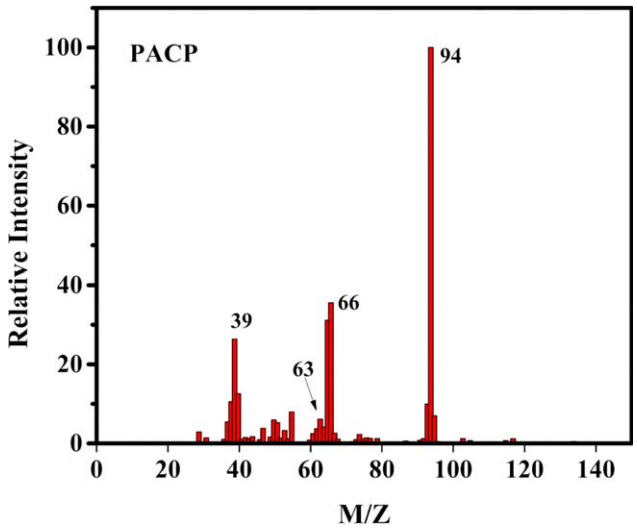

Figure 7. Py-GC/MS spectra of PACP. [Color figure can be viewed in the online issue, which is available at wileyonlinelibrary.com.]

PACP were mainly 2-allyphenol, 2-allyphenol derivatives and containing furan ring produces, which further indicated the allyl ether groups of PACP occurred Claisen rearrangement during the thermal pyrolysis process.

Table V shows the pyrolysis products of PET/5% PACP and PET/15% PACP, respectively. When PACP was incorporated into PET matrix, the main pyrolysis products were detected in the gaseous phase, such as benzene acid, divinyl terephthalate, and their substitution products, as listed in Table V. It was reported that the mechanism of PET degradation was a free radical process.[18,34,35] The free radical products, for example, $C_6H_5COO•$ and $C_6H_5COOCH_2CH_2•$, could generated during the degradation process.[35] As shown in Table V, the relative peak intensities of $C_6H_5COOCH_2CH_2OOP$, and $CH_3COC_6H_5COOOOP$ were 3.25% and 0.25%, respectively during the Py-GC/MS test of PET/5% PACP. This behavior could be explained that the decomposition products (PO_2) form PACP acted as a radical trap, which led to inhibit the free radical degradation of PET chain and suppressed combustion in gaseous phase. For the case of PET/15%PACP, the relative peak intensities of $C_6H_5COOCH_2CH_2OOP$, and $CH_3COC_6H_5COOOOP$ were 3.44% and 0.59%, respectively. Compared with PET/5% PACP, only slightly increase in the relative peak intensities of phosphorus-containing annihilated products of PET/15% PACP. It was well explaining that the flame retardance of PET/15% PACP (32.1 vol %) was no further enhanced.

On the basis of the investigation about the gas-phase products of the PET/PACP composites, it could be confirmed that the PACP can produce the phosphinylidyne free radicals, which could terminate the combustion. Therefore, the PET/ 5%PACP composites were the outstanding self-extinguishing thermoplastic material in the UL 94 tests, resulted from the flame-retardant action in gas phase.

Char Morphology of PET/PACP Composites

Just as organophosphorus flame retardants, the flame-retardant action of PACP may be expected in gas phase due to flame inhibition of fuel, and/or in the condensed phase due to involving of the macromolecules in charring process.[9,14–16,36] It was well known that the morphology and architecture of the char were very important for the condensed phase activity. To further explore the flame-retardant effect of PACP in solid phase, morphology, and architecture of the residual char after LOI testing was analyzed by SEM, and FTIR. Figure 8 presents the SEM images of the exterior and inner char residues of the samples. The char layer with the compact outer surface and many

Table V. Main Pyrolysis Products of PET/5%PACPand PET/15%PACP

PET/5%PACP			PET/15%PACP		
Time (min)	Products	Relative peak intensity (%)	Time (min)	Products	Relative peak intensity (%)
10.504	Vinyl benzoate	4.1	10.49	C_6H_5CN	0.35
11.829	Benzoic acid	46.6	11.001	Vinyl benzoate	1.4
11.938	Phenyl 4-ethylbenzoate	0.19	11.672	Benzoic acid	78.33
12.112	Vinyl trans-cinnamate	0.29	12.314	Biphenyl	0.64
12.187	Biphenyl	1.35	12.487	Methanol, oxo-, benzoate	2.13
12.35	Methanol, oxo-, benzoate	5.98	14.024	Pyrazine, 2,3-diethyl-5-methyl-	0.81
14.024	$CH_2CHOOCC_6H_4COOCHCH_2$	4.63	14.544	Benzaldehyde, 2,4,5-trimethyl-	4.73
14.296	Ethy 4-acetybenzoate	1.89	15.155	2-Prpenoic acid, 3-phenyl-	2.5
14.895	4-Vinybenzoic acid	0.43	15.742	Ethyl 4-cyanobenzoate	4.47
15.85	Benzoic acid, 2-(1-oxoprpyl)-	29.47	16.221	9H-Fluoren-9-one	0.61
16.133	9H-Fluoren-9-one	0.16	16.301	$C_6H_4COOCH_2CH_2OOP$	3.44
16.25	$C_6H_4COOCH_2CH_2OOP$	3.25	16.509	$CH_3OOCC_6H_4COOOOP$	0.59
16.43	$CH_3OOCC_6H_4COOOOP$	0.25			
16.506	Biphenul-2,2′-dialdehyde	0.17			
18.42	1,2-Ethandiol, dibenzote	1.24			

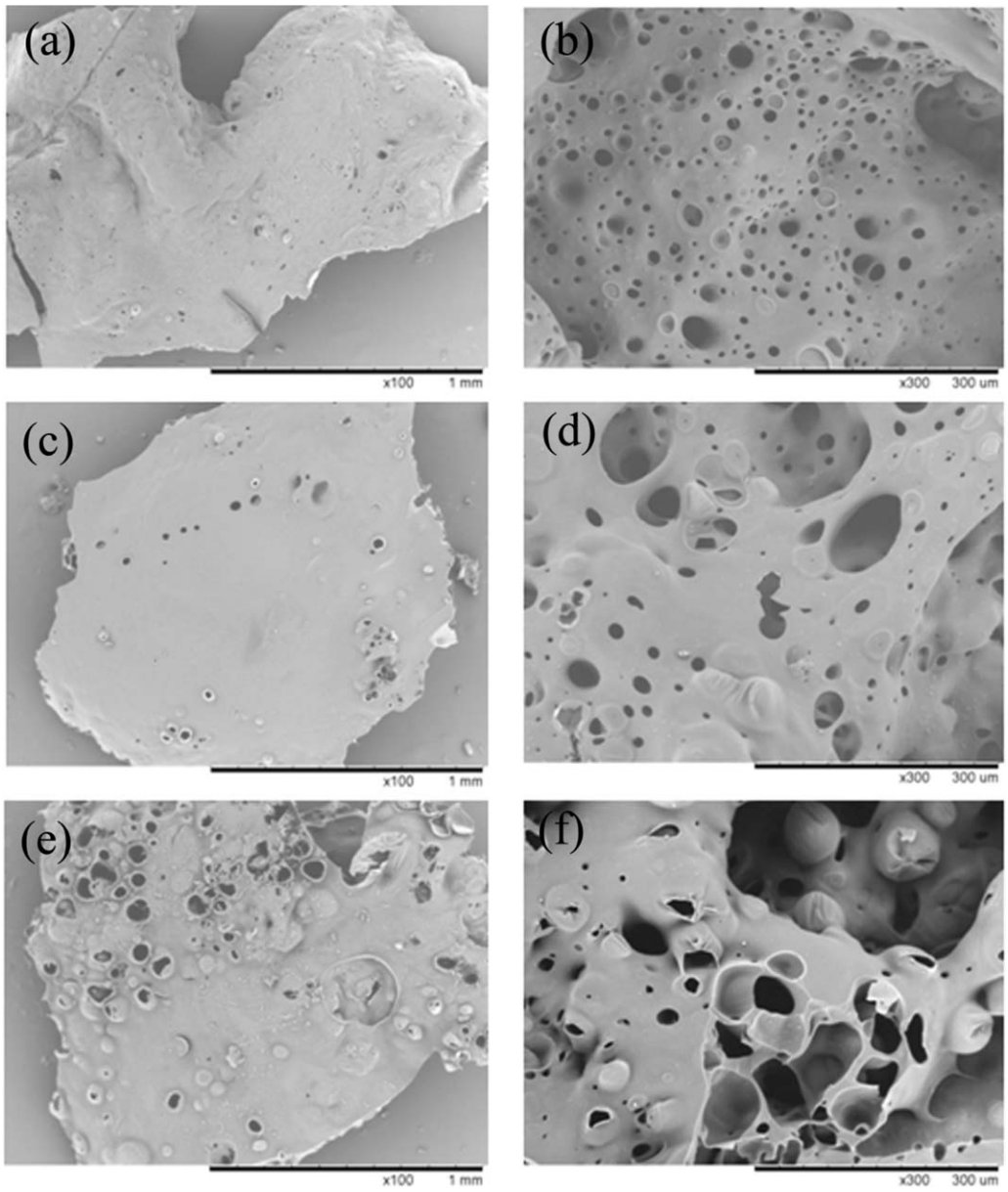

Figure 8. SEM images of PET/PACP composites char after LOI test: the outer and inner surface of PET/5%PACP (a, b), PET/10%PACP (c, d), and the outer and inner surface of PET/15%PACP (e, f).

uniform micro porous in the inner layer was observed, as shown in Figure 8(A−D), which acted as insulating barrier to prevent the oxygen and the feedback of heat from reaching the underling material during the process of combustion. On the contrary, there were vast quantity of large holes in the outer surface and inner char of PET/15%PACP as shown in Figure 8(E,F), which mean that the char layer is not compact enough to provide excellent heat and fuel insulation and protect the polymer matrix from attacking of the heat and fire. This result was agreed with the flame-retardant of the PET/5%PACP, PET/10%PACP and PET/15%PACP above tests.

The residues of neat PET, PET/5%PACP and PET/15%PACP composites after burning were investigated by FTIR to reveal the degradation reactions. Compared with the IR spectra of neat PET, as shown in Figure 9, the IR spectra of PET/5%PACP residues appeared the peak at 1710 cm^{-1} (the anhydride group) and a series of stronger absorption bands around 1600 and 1400 cm^{-1} (the cross-linking carbon-oxygen structure)[37] and 788 cm^{-1} (C_{Ar}-H deformation vibration) in the Figure 9. The absorption of peaks at 1163 cm^{-1} (P═O), 1072 cm^{-1} (P─OH), 901 cm^{-1}(O─P─O) and 885 cm^{-1} (O═P─O) were observed,[38,39] which were confirmed the presence of various phosphorus products. That is, the addition of 5 phpp PACP into PET matrix promoted the cross-linking char containing phosphorous during burning and acted as a protective barrier to separate heat and cut off oxygen. Meanwhile, the cross-linking char layers of PET/5%PACP enhanced the inhibition of melt-dripping properties of the composites during the UL 94

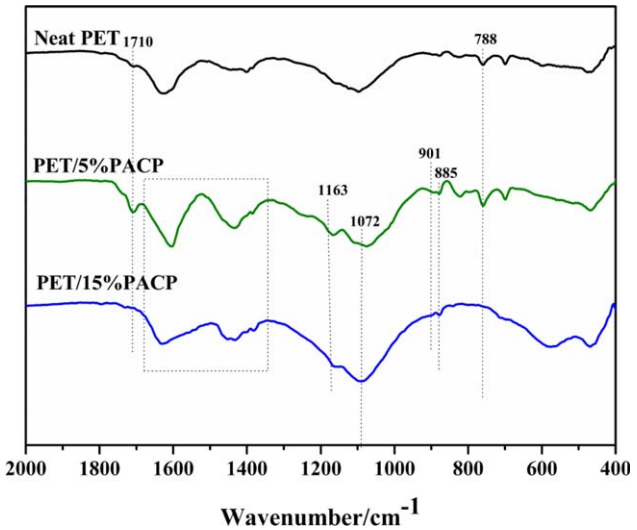

Figure 9. IR spectrum of residues of PET, PET/5%PACP and PET/15% PACP. [Color figure can be viewed in the online issue, which is available at wileyonlinelibrary.com.]

tests, only 1–2 melt-dripping appeared in the second 10s application of the burner.

The element analysis (EA) of the original and the residue of PET/PACP composites at 600°C in a Muffle Furnace for 5 min under nitrogen atmosphere was performed. As shown in Table VI, the residue rate of PET/5%PACP and PET/15%PACP were 23.53% and 30.92%, respectively. The content of C increased from 61.89 wt % to 82.15 wt % for PET/5%PACP after treatment, which might form more stable C structures,[40] such as C═C, etc. Meanwhile, it was found that the content of phosphorus in the char was significantly increased after the heating treatment. One reason was that thermal decomposition consumed lots of other elements (C, O, H, N) caused the accumulation of P element on the condensed phase.[40,41] That implied the formation of P-containing cross linking aromatic carbon during the thermal decomposition process. Obviously, the change tends for the main elements in the condensed phase were consistent with the results of the char residues after LOI tests in FTIR.

Furthermore, the maximum theoretical phosphorus content (P_{mt}) in the residue is calculated according to the following equation:[42]

$$P_{mt} = (P_o / \text{Residue rate}) \times 100\% \quad (1)$$

where P_o is the actual phosphorus content of the PET/PACP composites, which was tested by ICP-AES. The P_{air} is defined as the amount of phosphrous volatilized into the air, calculated by P_{mt} tacking off P_{char} (the actual phosphorous content in char residue after the treatment of Muffle Furnace). R is defined as the ration of P_{air} and P_{mt}. The P_{air} value of PET/5%PACP was 0.85 wt %, R of PET/5%PACP was 54.1%, indicating that a considerable amount of phosphrous volatilized into air. While, the P_{air} value of PET/15%PACP was 1.27 wt %, R of PET/15%PACP was 28.1%, suggesting that the majority of phosphorus remained in char residue. This result was consistent with the evolved gas analysis of PET/PACP composites. The structural integrity failure of carbon protection layer for PET/15%PACP composites (seen in SEM figures, such as holes or cracks) resulted into the release of the flammable volatiles, was no further improve the flame retardance, although the content of phosphorus in char residue was improved.

For PET/PACP system, based on the result of the flame retardancy mechanisms analysis in the gaseous and condensed phase, the flame-retardant activity of exothermic Claisen rearrangement PACP combined gas-phase with condensed-phase. The PACP could produce a large number of phosphorus-containing free radicals, which acted as the radical scavengers to combine with the free radical degradation of PET and fire inhibitors to scavenged H· and OH· in the flame. Moreover, according to the TGA tests and char morphology analysis, the hydrolysis of PACP was proposed to produce phosphorous acids at the right temperatures, enhancing a larger amount of compact and intact char residues in the condensed phase. The higher efficiency of per phosphorous atom in PACP was attributed to combine the activity of phosphorous flame retardance in gaseous phase with condensed phase. Thus, a concentration of 0.37 wt % phosphorus of PET/5%PACP was enough to increase the LOI value to 33.5 vol %.

Mechanical Properties and Crystallization Behaviors of PET/PACP Composites

To evaluate the influence of PACP flame retardants on the mechanical performance of PET matrix, the tensile strength, Yong' modulus, and elongation at break were measured. Neat PET showed a tensile strength of 38.47 MPa, Yong' modulus of 1819.05 MPa, and an elongation at break of 2.19%. As shown in Figure 10, incorporated 5 phpp PACP into PET matrix, the tensile strength was 29.67 MP, about 77.13% contrasted to that of neat PET. In addition, the Young's modulus of the PET/

Table VI. Residue Rate at 600°C in a Muffle Furnace for 5 min Under Nitrogen atmosphere and Elemental Components of PET/5%PACPand PET/15%PACP Measured by EA

			Element component (wt %) (Found)		
Samples		Residue Rate (%)	C	N	P
PET/5%PACP	Original	23.53	61.89	0.07	0.37
	Residue		82.15	0.08	0.72
PET/15%PACP	Original	30.92	61.72	0.34	1.03
	Residue		76.24	0.29	2.06

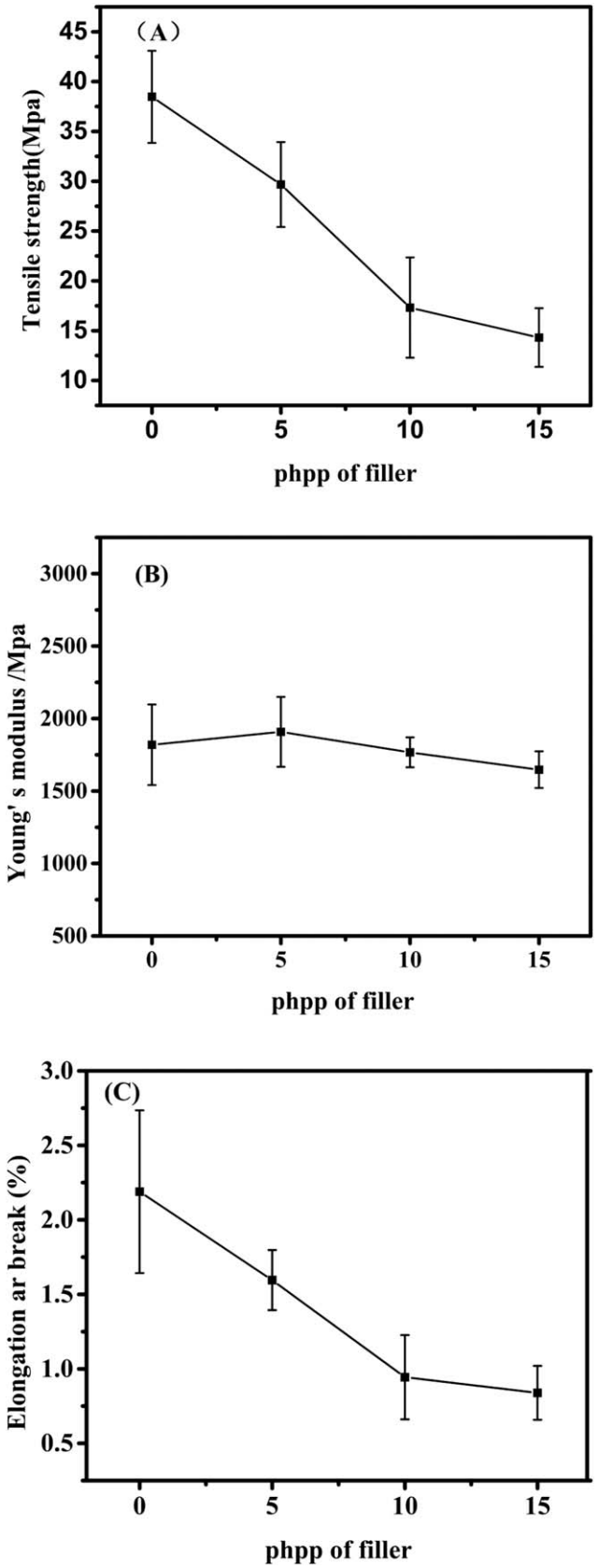

Figure 10. Mechanical properties of PET/PACP composites as a function of PACP content.

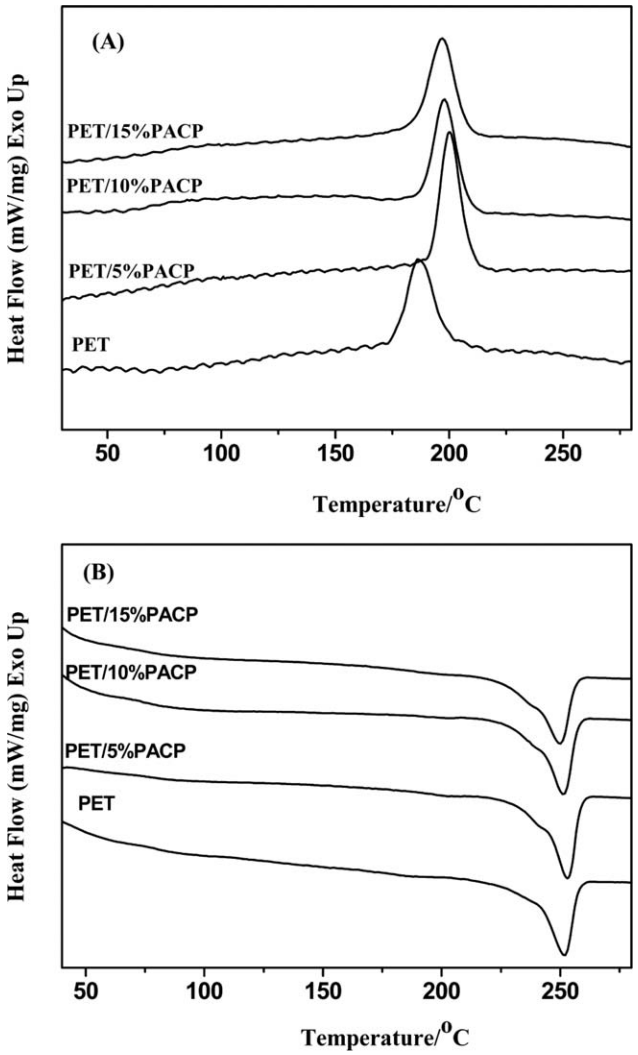

Figure 11. DSC thermograms of PET and the blends: (A) cooling scans and (B) heating scans.

5%PACP was 1908.32 MPa, which was higher than that of neat PET. It was found that the PACP was a big favor in keeping the mechanical properties of the composite at low content. However, as shown in Figure 10, both tensile strength and elongation at breaking of PET/10%PACP and PET/15%PACP exhibited a sudden drop, as well as the Young's modulus of them decreased. A possible explanation for the decrease in tensile strength with the increase in PACP content was that the formed large PACP domains would tend to act as the structural defects and would eventually decreased the mechanical properties.

Table VII. DSC Data of PET and the Blends Samples

Sample	T_C (°C)	$\triangle H_C$ (J/g)	T_m (°C)	$\triangle H_m$ (J/g)
Neat PET	186.2	33.87	251.9	31.75
PET/5%PACP	200.2	41.95	253.0	37.96
PET/10%PACP	197.9	36.68	251.4	36.65
PET/15%PACP	197.0	35.80	249.9	34.74

In general, the presence of foreign bodies in the polymer melt increases the crystallization rate, crystallization temperature and degree of crystallinity, which can improve the thermal, mechanical, and optical properties of semicrystalline polymers.[43,44] Thus, the crystallization behaviors of neat PET and PET/PACP composites were investigated by successive DSC analysis. Figure 11 shows the first cooling scans and the second heating scans of neat PET and PET/PACP, the detailed information is summarized in Table VII. Compared with neat PET, the crystallization peaks of the PET/CPs became sharp and narrow, for instance, the T_C of PET/5%PACP increased from 186.2°C (T_C of PET) to 200.2°C, corresponding $\triangle H_C$ increased from 33.87 J/g ($\triangle H_C$ of PET) to 41.95 J/g during the cooling process. The results indicated that the crystalline of PET/PACP composites was strengthened. It was caused by the phenyl group-containing PACP was a kind of heterogeneous nucleation agent.[43–45] Meanwhile, a slight decrease of the *Tc* and $\triangle H_C$ of PET/PACP appeared with the increase of PACP contents, for instance, the *Tc* of PET/15%PACP decreased from that of PET/5%PACP (200.2°C) to 197.0°C, $\triangle H_C$ from 41.95 J/g to 35.80 J/g as well. This implied that incorporating more PACP into PET matrix weakened the crystalline behavior of PET/PACP composites. When the low filler content (5 phpp) was introduced, the tensile strength of PET/PACP composite was retained and Young's modulus of which was increased. It was induced by the better crystallization performance in the PET matrix, in the other word, the chain segments of PET tend to crystallize and arrangement more order, which could form more physical network structures and increase the entanglement of the polymer chain. In addition, the T_m and $\triangle H_m$ of PET/PACP composites slightly increased contrast to that of neat PET. Through analysis of crystallization behaviors of PET/PACP composites, one simple conclusion was summarized that, the crystallization behaviors of PET/PACP composites could be promoted by the incorporated PACP into PET matrix with a relatively small amount and the mechanical properties of which could meet the requirements during application. A further intensive study is still necessary to recover the loss mechanical properties of PET/5%PACP composite through the combination of different nanoparticles because of the outstanding properties of these nanocomposites, like mechanical, thermal and flame-retardant performance.

CONCLUSIONS

A high efficiency cyclophosphazen flame-retardant (PACP) was successfully synthesized by three-step method, which can retard the PET to burn by gas phase and solid phase mechanism. There is a little effect on the mechanical properties of the PET. The prepared PET/PACP composites by this work exhibits a broad prospect for textile materials applications as a nonflammable fabrics.

ACKNOWLEDGMENTS

The authors gratefully acknowledge the funding by the National High-tech Research and Development Program (863 Program) under grant 2007AA03Z336 and 2013AA06A307, and the Program for New Century Excellent Talents in University under grant NCET-07–0174.

REFERENCES

1. Horrocks, A. R. *Polym. Degrad. Stab.* **2011**, *96*, 377.
2. Joseph, P.; Tretsiakova-Mcnally, S. *Polym. Adv. Technol.* **2011**, *22*, 395.
3. Lu, S. Y.; Hamerton, I. *Prog. Polym. Sci.* **2002**, *27*, 1661.
4. Cheung, M. F.; Carduner, K. R.; Golovoy, A.; Oene, H. V. *J. Appl. Polym. Sci.* **1990**, *40*, 977.
5. Reemtsma, T.; Quintana, J. B.; Rodil, R.; García-López, M.; Rodríguez, I. *Trac-Trend Anal. Chem.* **2008**, *27*, 727.
6. Veen, I.; Boer, J. *Chemosphere* **2012**, *88*, 1119.
7. Martínez-Carballo, E.; González-Barreiro, C.; Sitka, A.; Scharf, S.; Gans, O. *Sci. Total Environ.* **2007**, *388*, 290.
8. Regnery, J.; Püttmann, W. *Water Res.* **2010**, *44*, 4097.
9. Mihajović, I. In Flame Retardants Polymer Blends, Composites and Nanocomposites; Visakh, P. M.; Arao, Y., Eds.; Springer: Switzerland, **2015**; Chaper 4, p 79.
10. Wang, Y. Z. In Advances in Fire Retardant Materials; Horrocks, A. R.; Price, D., Eds.; Woodhead Publishing: Cambridge, England, **2008**; Chapter 4, p 76.
11. Song, P.; Shen, Y.; Du, B.; Peng, M.; Shen, L.; Feng, Z. *ACS Appl. Mater. Inter.* **2009**, *1*, 452.
12. Salaün, F.; Creach, G.; Rault, F.; Griaud, S. *Polym. Degrad. Stab.* **2013**, *98*, 2663.
13. Doğan, M.; Erdoğan, S.; Bayramh, E. *J. Therm. Anal. Calorim.* **2013**, *112*, 871.
14. Qian, L.; Feng, F.; Tang, S. *Polymer* **2014**, *55*, 95.
15. Kilinc, M.; Cakal, G. O.; Bayram, G.; Eroglu, I.; Özkar, S. *J. Appl. Polym. Sci.* **2015**, *132*, 42016.
16. Sahyoun, J.; Bounor-Legaré, V.; Ferry, L.; Sonnier, R.; Bonhommé, A.; Cassagnau, P. *Polym. Degrad. Stab.* **2015**, *115*, 117.
17. Li, J.; Pan, F.; Xu, H.; Zhang, L.; Zhong, Y.; Mao, Z. *Polym. Degrad. Stab.* **2014**, *110*, 268.
18. Zhang, X.; Zhong, Y.; Mao, Z. *Polym. Degrad. Stab.* **2012**, *97*, 1504.
19. Kuan, J. F.; Lin, K. F. *J. Appl. Polym. Sci.* **2004**, *91*, 697.
20. Guo, Y. N.; Ming, J. Y.; Li, C. Y.; Qiu, J. J.; Tang, H. Q.; Liu, C. M. *J. Appl. Polym. Sci.* **2011**, *121*, 3137.
21. Lim, H.; Chang, J. Y. *J. Mater. Chem.* **2010**, *20*, 749.
22. Herrera-González, A. M.; García-Serrano, J.; Pelaz-Cid, A. A.; Montalvo-Sierra, I. *IOP Conf. Ser.: Mater. Sci. Eng.* **2013**, *45*, 012008.
23. Guo, Y. N.; Zhao, C.; Liu, S. Z.; Li, D.; Wang, S. J.; Qiu, J. J.; Liu, C. M. *Polym. Bull.* **2009**, *62*, 421.
24. Bagnell, L.; Cablewski, T.; Strauss, C. R.; Trainor, R. W. *J. Org. Chem.* **1996**, *61*, 7355.
25. Shin, Y. J.; Ham, Y. R.; Kim, S. H.; Lee, D. H.; Kim, S. B.; Park, S. P.; Yoo, Y. M.; Kim, J. G.; Kwon, S. H.; Shin, J. S. *J. Ind. Eng. Chem.* **2010**, *16*, 364.
26. Fantin, G.; Medici, A.; Fogagnilo, M.; Pedrini, P.; Gleria, M.; Bertani, R.; Facchin, G. *Eur. Polym. J.* **1993**, *29*, 1571.
27. Medici, A.; Fantin, G.; Pedrini, P.; Gleria, M.; Minto, F. *Macromolecules* **1992**, *25*, 2569.
28. Han, X.; Armstrong, D. W. *Org. Lett.* **2005**, *7*, 4205.

29. Chang, H. C.; Lin, C. H.; Lin, H. T.; Dai, S. A. *J. Polym. Sci. Part A: Polym. Chem.* **2012**, *50*, 1008.
30. Lyon, R. E.; Safronava, N.; Quintiere, J. G.; Stoliarov, S. I.; Walters, R. N.; Crowley, S. *Fire Mater.* **2014**, *38*, 264.
31. Yang, C. Q.; He, Q.; Lyon, R. E; Hu, Y. *Polym. Degrad. Stab.* **2010**, *95*, 108.
32. Badia, J. D.; Martinez-Felip, A.; Santonia-Blaco, L.; Ribes-Greus, A. *J. Anal. Appl. Pyrol.* **2013**, *99*, 191.
33. Mao, Z.; Li, J.; Pan, F.; Zeng, X.; Zhang, L.; Zhong, Y.; Sui, X.; Xu, H. *Ind. Eng. Chem. Rec.* **2015**, *54*, 3788.
34. Zhang, J.; Ji, Q.; Zhang, P.; Xia, Y.; Kong, Q. *Polym. Degrad. Stab.* **2010**, *95*, 1211.
35. Botelho, G.; Queirós, A.; Liberal, S.; Gijsman, P. *Polym. Degrad. Stab.* **2001**, *74*, 39.
36. Balabanovich, A. I.; Pospiech, D.; Häußler, L.; Harnisch, C.; Döring, M. *J. Anal. Appl. Pyrol.* **2009**, *86*, 99.
37. Han, X.; Zhao, J.; Liu, S.; Yuan, Y. *RSC Adv.* **2014**, *4*, 16551.
38. Zhang, X.; Zhang, L.; Wu, Q.; Mao, Z. *J. Ind. Eng. Chem.* **2013**, *19*, 993.
39. Shao, Z.; Deng, C.; Tan, Y.; Chen, M.; Chen, L.; Wang, Y. *ACS Appl. Mater. Interfaces* **2014**, *6*, 7363.
40. Chen-Yang, Y. W.; Lee, H. F.; Yuan, C. Y. *J Polym. Sci. Part A: Polym. Chem.* **2000**, *38*, 972.
41. Zhang, W.; Li, X.; Yang, R. *Polym. Degrad. Stab.* **2014**, *99*, 298.
42. Zhang, Y.; Ni, Y.; He, M.; Wang, X.; Chen, L.; Wang, Y. *Polymer* **2015**, *60*, 50.
43. Pan, P.; Liang, Z.; Cao, A.; Inoue, Y. *ACS Appl. Mater. Interfaces* **2009**, *1*, 402.
44. Libster, D.; Aserine, A.; Garti, N. *Polym. Adv. Technol.* **2007**, *18*, 685.
45. Li, J.; Liang, Q.; Lu, A.; Luo, S.; Liu, T.; Liu, Y.; Shi, D.; Liu, T. *Polym. Compos.* **2013**, *34*, 867.